Climatic and phenological controls on coherent regional interannual variability of carbon dioxide flux in a heterogeneous landscape

Ankur R. Desai[1]

Received 4 May 2010; revised 13 August 2010; accepted 24 August 2010; published 3 December 2010.

[1] The climate sensitivity of plant seasonal life cycles, or phenology, may impart significant carbon cycle feedbacks on climatic change. Analysis of interannual ecosystem carbon exchange provides one way to assess this climate sensitivity. Multiyear eddy covariance carbon dioxide flux observations from five different ecosystems (deciduous forest, northern hardwood mixed forest, old-growth forest, shrub wetland, and mixed wetland-forest) in the Upper Great Lakes, United States, located within 400 km of each other and exhibiting coherent interannual variability, were used to parameterize a simple ecosystem model. The model, when properly constrained with an interannual sensitive cost function, was able to explain a significant proportion of the interannual variation of carbon fluxes in all ecosystems except the old-growth forest. The results reveal that spring or autumn climate thresholds impact annual carbon uptake, though the magnitude and strength varied by site. When the model was forced to maintain the same climate-phenology relationship across the five sites, most of the interannual variability could still be explained except at the old-growth forest and the forest farthest in distance from the others. These results suggest that at least for this region, coarse spatial resolution carbon-climate models could likely specify general climate-phenological relationships at grid scales on order of 100 km without appreciably sacrificing ability to model interannual carbon cycling.

Citation: Desai, A. R. (2010), Climatic and phenological controls on coherent regional interannual variability of carbon dioxide flux in a heterogeneous landscape, *J. Geophys. Res.*, *115*, G00J02, doi:10.1029/2010JG001423.

1. Introduction

[2] One key to understanding impacts of the terrestrial carbon cycle on future climate change is better diagnosis of climatic controls on interannual variability (IAV) of land-atmosphere carbon dioxide net ecosystem exchange (NEE). This is especially the case in temperate and boreal forests where IAV is large [*Yuan et al.*, 2009] and strongly linked to climate variability [e.g., *Barr et al.*, 2006; *Chen et al.*, 1999; *Goulden et al.*, 1996; *Hollinger et al.*, 2004; *Sierra et al.*, 2009]. Large IAV could, for example, lead to reduced long-term carbon accumulation in some forests, due to the impact of disturbance-driven respiration pulses [*Sierra et al.*, 2009]. Despite its importance, observed IAV of NEE in these biomes is difficult to simulate in ecosystem models, which are better tuned to capture diurnal, seasonal, and successional patterns [*Ricciuto et al.*, 2008; *Urbanski et al.*, 2007; *Stoy et al.*, 2009].

[3] Currently, we lack a strong physical basis for many of the complex interactions that exist in terrestrial systems at this timescale [*Bonan*, 2008; *Stoy et al.*, 2009]. For example, while annual NEE typically declines with latitude in temperate regions, relative IAV increases in deciduous forests and declines in evergreen forests, a result that is difficult to explain [*Yuan et al.*, 2009]. In several grasslands, it was noted that sensitivity of plant productivity to climate drivers varied year-to-year [*Polley et al.*, 2010]. This result is similar to findings of *Richardson et al.* [2007] who argued that biotic, not climate, variability was the primary cause of decadal flux variability in a spruce forest.

[4] Still, we lack understanding about what spatial scales do we expect to see coherence in interannual variability. Identifying such would enable specification of optimal spatial resolution for specifying climate-ecosystem relationships in land-atmosphere models. One promising avenue of research for better modeling of regional ecosystem model IAV is improved simulation of climate sensitivity in plant phenological life cycles [*Peñuelas et al.*, 2009]. Phenology links climate anomalies, especially in the shoulders of the plant growing season, to plant biogeochemistry [*Morisette et al.*, 2009; *Piao et al.*, 2008].

[5] Recent climatic warming leading to advances in spring flowering and leaf timing has been noted in many parts of the globe [*Linderholm*, 2006], especially in Europe [*Menzel and Fabian*, 1999; *Stöckli and Vidale*, 2004] and North America [*Myneni et al.*, 1997; *White et al.*, 2009], and across diverse ecosystems including temperate forests [e.g., *Richardson et al.*, 2006; *Vitasse et al.*, 2009] and Mediterranean shrub-

[1]Department of Atmospheric and Oceanic Sciences, University of Wisconsin-Madison, Madison, Wisconsin, USA.

0148-0227/10/2010JG001423

Table 1. Location and Types of Colocated Eddy Covariance Flux Towers and Time Periods Analyzed in This Study Along With Their Mean Annual NEE and Uncertainty, σ IAV, Postfiltering Total Gap Fraction, and Reference[a]

Name	Location	Type	Years	NEE (gC m^{-2} yr^{-1})	IAV (gC m^{-2} yr^{-1})	Percent Gaps	Reference
US-WCr	45°48′N, 90°5′W	Northern hardwood mature forest	2000–2006	−380 ± 29	149	51%	*Cook et al.* [2004]
US-UMB	45°34′N, 84°43′W	Deciduous broadleaf mature forest	1999–2003	−284 ± 22	43	39%	*Gough et al.* [2008]
US-Syv	46°14′N, 89°21′W	Old-growth mixed forest	2002–2006	1 ± 18	112	48%	*Desai et al.* [2005]
US-Los	46°5′N, 89°59′W	Shrub fen wetland	2001–2006	−84 ± 10	16	32%	*Sulman et al.* [2009]
US-PFa	45°57′N, 90°16′W	Mixed regional footprint	1997–2005	111 ± 21	67	28%	*Ricciuto et al.* [2008]

[a]Data gaps were strongly skewed toward nighttime data due to low turbulence screening criteria.

lands [e.g., *Gordo and Sanz*, 2010]. Climate records hint at shifts in both phase and amplitude of the annual temperature [*Stine et al.*, 2009], suggesting that links between phenology and climate will likely have significant impacts on ecosystem productivity with ensuing anthropogenic climate change. The impact of warm springs and longer growing season lengths on carbon uptake has been well noted at several sites [*Barr et al.*, 2006; *Chen et al.*, 1999; *Churkina et al.*, 2005; *Dragoni et al.*, 2010; *Goulden et al.*, 1996; *Hollinger et al.*, 2004], but ecosystem models that can capture this impact on IAV are elusive [*Baldocchi et al.*, 2005].

[6] One way to advance our understanding is to develop and test ecosystem models constrained by multiyear observations that connect phenology, carbon cycling, and climate at multiple sites. Long-term eddy covariance flux towers, which directly observe NEE of ecosystems over multiple years, are particularly well suited for testing how well models of phenology capture carbon cycle IAV [*Richardson et al.*, 2009], though only a few studies have used multiple flux towers [*Baldocchi et al.*, 2005; *Churkina et al.*, 2005] and none focused on multiple towers in one region. Coherent IAV has been observed across a set of flux towers in a similar climate and biome [*Desai et al.*, 2008], but there has been limited success in modeling this IAV. Here, I ask to what extent can the observed IAV be explained by a simple climate sensitive model of plant phenology and what does it imply for methods to improve modeling of ecosystem IAV?

[7] To investigate this question, a simple ecosystem model was developed and parameterized using Bayesian techniques against multiyear flux tower data observed in five ecosystems that span a range of ecoystem types from mixed forests to hardwood forests to shrub wetlands, where we would not expect a priori coherent interannual carbon cycle responses. Estimating parameters in models involves a cost function that is typically based on least squares comparison of hourly or daily modeled and observed NEE. However, this cost function formulation may mute the information content of IAV in observations. To test this assertion, an alternative IAV-sensitive formulation of the cost function was also applied as part of the parameterization. Finally, to investigate controls on synchronous forcing, model parameterization was further modified to force spatial convergence on phenological parameters. Findings from these investigations are used to discuss implications for environmental controls and spatial coherence of regional IAV.

2. Data and Methods

2.1. Site and Data Description

[8] Five eddy covariance flux towers in the temperate-boreal transition region of the Upper Great Lakes were analyzed in this study (Table 1). The sites, which included three forests of different age classes and types, one shrub wetland, and one tall tower regional mixed forest-wetland footprint, are located within 400 km of each other (Figure 1). Each site has at least five years of flux and meteorological data, and have been previously analyzed and described in an upscaling study [*Desai et al.*, 2008]. Four of the sites (US-WCr, US-Syv, US-Los, and US-PFa) are within 150 km of each other in north central Wisconsin/upper Michigan, while the fifth site, US-UMB, is in northern Lower Michigan. Of the forest sites, two are mature age class (US-WCr and US-UMB), and one is old-growth (US-Syv). While US-WCr is a northern hardwood forest, dominated by maple-beech-basswood cover, US-UMB, on sandier soil, is dominated by more of an aspen-oak mix. US-Syv is more reflective of presettlement conditions, with a mixed maple-hemlock tree cover. The wetland site is a short-stature shrub alder-willow fen. The tall tower is a 447 m radio tower with flux measurements at three heights. For the purposes of this comparison, the fluxes from the three levels of the tall tower were combined in an optimal selection strategy, as described by *Davis et al.* [2003], to produce a single "regional" NEE. This regional NEE footprint sampled a range of mature northern hardwood forests, early aspen forests, open bogs, and shrub wetlands.

[9] Meteorological data from each site were acquired and gap-filled using a combination of nearest neighbor and moving-window ensemble diurnal average techniques [*Desai et al.*, 2008]. Eddy covariance and storage fluxes of CO_2 observed with closed-path infrared gas analyzers and 3-D sonic anemometry were used to compute NEE at each site. Standard

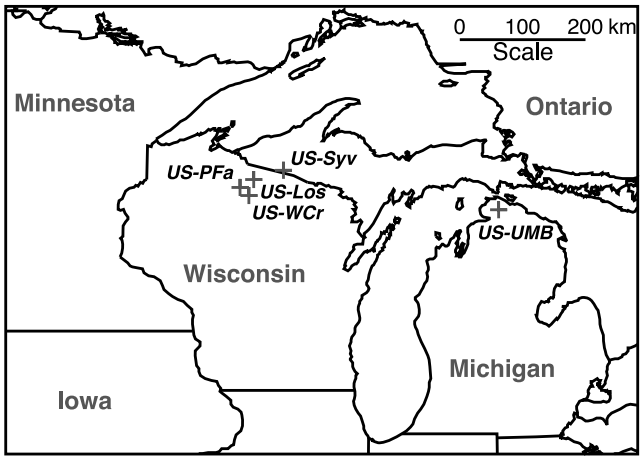

Figure 1. Map of north central United States showing location of the five flux tower sites used in this study.

Table 2. Model Parameters Definitions, Prior Values, and Acceptable Posterior Parameter Ranges Used by the IFUSE Model and MCMC Parameterization

Name	Definition	Value
	Fixed Parameters	
k	Light extinction coefficient	0.5 fixed
LAI_{min}	Minimum leaf area	US-WCr 0.0, US-UMB 0.0, US-Syl 0.5, US-Los 0.0, US-PFa 0.5
LAI_{max}	Maximum leaf area	US-WCr 5.3, US-UMB 3.7, US-Syl 4.1, US-Los 4.9, US-PFa 3.7
	Phenology Parameters	
α	Leaf on (L_{ON}) slope	0.05 (0.05–0.5)
GDD_{thresh}	Growing degree day threshold	200 (10–400)
β	Leaf off (L_{OFF}) slope	0.1 (0.05–0.5)
$TEMP_{thresh}$	Soil temperature threshold	4 (0–20)
	Photosynthesis Parameters	
LUE	Light use efficiency	0.25 (0–1)
T_{min}	Minimum photosynthetic temperature	0 (−15–10)
T_{opt}	Optimum photosynthetic temperature	15 (5–40)
VPD_{max}	Maximum photosynthetic VPD	3000 (0–20000)
VPD_{min}	Minimum photosynthetic VPD	100 (0–2000)
	Respiration Parameters	
r_s	Basal maintenance respiration	2 (0.1–5)
r_v	Basal growth respiration	2 (0.1–5)
b_1	Maintenance respiration rate	0.03 (0–0.5)
b_2	Growth respiration rate	0.03 (0–0.25)
b_3	Leaf respiration fraction	0.05 (0–0.25)

flux computation methods at each site were relatively similar [*Desai et al.*, 2008] and fluxes computed by these codes have compared favorably to the Ameriflux "gold" standard, a network-wide blind data processing protocol. Common techniques were used to screen for low turbulence conditions and gap filling of data gaps that occur due to low turbulence or instrument failure [*Desai et al.*, 2005]. The gap-filling technique compared well with other standard techniques used by the flux tower community [*Moffat et al.*, 2007]. All fluxes were computed at the half-hourly scale, except for US-PFa, which used an hourly scale owing to the taller height. For assimilation into the model, all flux and meteorological data were averaged across day and night periods, similar to the method of *Sacks et al.* [2006]. Using half-daily summed fluxes reduces impact of random turbulent flux error on data assimilation, but retains the nocturnal respiration signal. Summed half-daily flux integrals whose hours were more than 25% gap-filled were discarded for data assimilation to minimize artifacts arising from model-model comparison.

2.2. Model Description

[10] A simple ecosystem model, the Interannual Flux Tower Upscaling Experiment (IFUSE), was parameterized against all site data. The model consisted of 17 total parameters (Table 2), of which 3 were fixed for each site, 10 were optimized at each site, and four phenology parameters were either optimized at each site separately (asynchronous mode) or jointly for all sites (synchronous mode). The model was run with a half daily (day/night) adaptive length time step, which has been shown to be well suited for parameter optimization against flux tower NEE [*Sacks et al.*, 2006].

[11] At each time step, the model applied environmental forcing of canopy air temperature (T_a), 5 cm soil temperature (T_s), photosynthetic active radiation (PAR), and vapor pressure deficit (VPD) to estimate gross primary production (GPP), ecosystem respiration (ER), and NEE in gC m^{-2} time $step^{-1}$ and leaf area index (LAI) in m^2 m^{-2}. GPP was estimated using a five-parameter light, temperature, and VPD limited modified light use efficiency equation:

$$GPP = LUE \cdot \left(1 - e^{-k \cdot LAI}\right) PAR \left(\frac{T_a - T_{\min}}{T_{opt} - T_{\min}}\right) \cdot \left(\frac{VPD_{\max} - VPD}{VPD_{\max} - VPD_{\min}}\right) \quad (1)$$

where LUE, k, T_{min}, T_{opt}, VPD_{max}, and VPD_{min} are model parameters as described in Table 2.

[12] To calculate LAI, leaf phenology of emergence and senescence was modeled with a two-parameter sigmoidal relationship. The phenology model used here consisted of the well established accumulated growing degree days base 10 C (GDD) approach for midpoint of leaf emergence and a 5 cm soil temperature threshold for midpoint of leaf senescence, models which have been shown to explain much of the variation in canopy development for northern forests [*Baldocchi et al.*, 2005; *Richardson et al.*, 2006]. Canopy fraction with evergreen vegetation was simulated by preventing LAI to decline beyond a minimum threshold (LAI_{min}), leading to:

$$\begin{cases} LAI = LAI_{\min} + \left[(LAI_{\max} - LAI_{\min}) L_{spring} L_{fall}\right] \\ L_{spring} = \frac{1}{e^{-\alpha\left(DOY - \frac{L_{on}}{2}\right)}}; L_{fall} = 1 - \frac{1}{e^{-\beta\left(DOY - \frac{L_{off}}{2}\right)}} \\ L_x = \frac{L_x - \min(L_x)}{\max(L_x) - \min(L_x)}; x = spring/fall \\ L_{on} = DOY|_{GDD > GDD_{Thresh}}; L_{off} = DOY|_{T_s < T_{Thresh} \cup L_{spring} > 0.99} \end{cases} \quad (2)$$

where LAI_{min}, LAI_{max}, α, β, GDD_{thresh}, and T_{thresh} are model parameters (Table 2). L_{spring} and L_{fall} describe the variation of

LAI around the leaf on (L_{on}) or leaf off (L_{off}) day of year (DOY). Both of these functions were further normalized to vary between 0 and 1 and then multiplied together, thus allowing LAI to vary between LAI_{min} and LAI_{max}. Consequently, interannual variability in LAI is quite muted in this model, which allowed this model to focus on the role of growing season length (G_{SL}) on IAV of NEE.

[13] ER was estimated with five parameters that control respiration rates in three soil pools sensitive to T_s, T_a, and GPP:

$$ER = \left[r_s \cdot e^{b_1(T_s-15)}\right] + \left[r_v \cdot e^{b_2(T_a-15)}\big|_{GPP>0}\right] + \left[b_3 \cdot GPP_{DOY-1}\right] \quad (3)$$

where r_s, r_v, b_1, b_2, and b_3 are model parameters (Table 2). The first term represents the combined effects soil heterotrophic and plant maintenance respiration. The second term, which is only present when GPP is positive, represents plant growth respiration (or alternatively, the change in respiration sensitivity in growing versus dormant seasons), while the final term, is a fraction of the previous day GPP, representing autotrophic respiration of newly assimilated carbohydrate and allows for GPP lag effects in the model. These formulations were chosen to represent the dynamics that could likely be resolved from NEE measurements, as opposed to a more mechanistic, but also more parameter intensive and pool sensitive model of respiration.

[14] NEE was computed as the residual between ER and GPP. The model was designed to be purposefully simple so as to capture the key diurnal and season dynamics typically seen in NEE observations while limiting the number of parameters. By avoiding specification of soil and biomass pools outside of leaves, the model removed one of the largest sources of uncertainty and equifinality in estimating model parameters from flux data [*Luo et al.*, 2009]. This structure implied that soil pools were assumed to be steady state relative to the fluxes, which is generally a reasonable assumption for mature, established secondary succession ecosystems. Since the goal was simulation of daily to interannual NEE at timescales less than a decade (i.e., < 10% of a temperate hardwood forest successional cycle), this assumption implied that short-term variations in NEE were driven entirely by the response of ER and GPP to climate. Given the mesic climate of the region, influences of precipitation and moisture variability were assumed to be minimal. The impact of these assumptions on interpretation of results is provided in the discussion.

2.3. Model Parameterization

[15] Free parameters of the model (phenology, photosynthesis and respiration parameters in Table 2) were estimated using a Markov Chain Monte Carlo (MCMC) estimator [*Braswell et al.*, 2005] with the Metropolis-Hasting algorithm [*Metropolis and Ulam*, 1949]. In this approach, free parameters were randomly perturbed across a range of reasonable prior values, assuming a uniform distribution (Table 2). New parameter sets were "accepted" when a cost function indicated better fit of model to data, and occasionally when not, so as to avoid local minima. Multiple chains (six, in this study) were built from random locations in parameter space and iterated until a convergence criterion is reached, usually within 50,000 iterations. Iteration sizes were chosen to be arbitrarily large, so as to oversample the parameter space. The best chain was then propagated forward another 70,000 iterations, and a subset of the final 80,000 iterations were saved as "accepted" parameter sets based on the acceptance criterion. Best model output and variance were computed from the model output of these accepted parameter sets. More details of the general approach are provided by *Braswell et al.* [2005].

[16] The first five years of half-daily NEE observations for each site were used in the MCMC cost function to minimize model-data mismatch. The cost function can be written as:

$$L_D = \prod_{i=1}^{n} \frac{1}{\sqrt{2\pi\sigma}} e^{\frac{-(x_i-\mu_i)^2}{2\sigma^2}} \quad (4)$$

where L_D is the likelihood to be maximized, x_i is observed half-daily NEE, u_i is model NEE, and σ^2 is data error with respect to model structure, which was computed as the mean sum of square deviations between x_i and u_i [*Sacks et al.*, 2006]. To improve numerical stability, this equation was computed as the log likelihood, allowing the product function to be written as a sum. Additionally, to test whether the cost function biases how well the model identifies parameters responsible for determining carbon flux IAV, equation (4) was further modified to account for both fast (half-daily) and slow (annual) variations in NEE:

$$\begin{cases} L_y = \prod_{i=1}^{n} \frac{1}{\sqrt{2\pi\sigma}} e^{\frac{-\left(x_i^m-\mu_i^m\right)^2}{2\sigma^2}} \\ x_i^m = \sum_{j=i-DOY}^{i} x_i; \mu_i^m = \sum_{j=i-DOY}^{i} \mu_i \\ L = L_D L_y \end{cases} \quad (5)$$

where L_y is a likehood for annual NEE, and x_i^m is observed cumulative NEE from the start of the year to point i, and u_i^m is the equivalent for the model. The new cost function is then the product of the two likelihoods. Thus the model trades fit at the daily scale for fits at the annual scale, with the assumption that accepted parameters sets would be Pareto optimal for both. Cumulative NEE was used instead of annual NEE to allow for both the daily and annual to have roughly the same weight and also to prevent the model from fitting annual NEE with a poor seasonal pattern. The expectation is that this cost function may improve model reproduction of seasonal NEE and IAV without significant loss in explaining short-term variation. While L_d was weighted to account for the influence of gap-filled data by removing half-daily NEE sums with more than 25% gap-filled, L_y included all NEE to create well formed NEE integrals. In most cases, this did not add significantly more points or appear to bias results.

[17] In addition to the two cost functions above, an alternate optimization was performed where phenology parameters (Table 2) were forced to be the same for all five sites. In this "synchrony" setup, the parameter optimization was run in tandem at all five sites, such that the four phenology parameters were optimized to be the same at all five sites, while the other ten parameters were allowed to vary by site. Computationally, this was simply performed by concatenating arrays of flux and forcing data for all sites, with 5 sets of 10 independent parameters (50), and 4 codependent parameters.

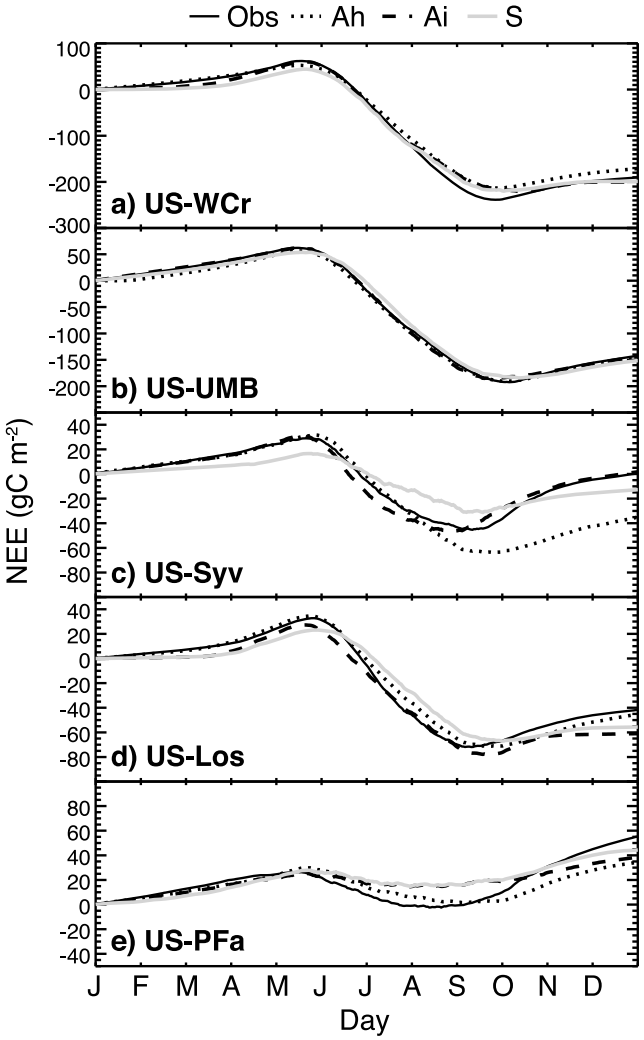

Figure 2. Ensemble average cumulative daily NEE for observations, and the three model experiments (A_H, A_I, and S). Averages were performed over the observed record noted in Table 1. The model generally captured the seasonal pattern of NEE at all sites, with worst performance at US-Syv and US-PFa. Observed and model uncertainty is not shown to preserve clarity, but generally fall within 10% of any observation.

Thus a single MCMC run estimated 54 parameters, instead of 14 at a time for each site. To compensate for the larger number of parameters, the number of chains was increased to 20 and total iterations to 432,000 (with 144,000 spin-up iterations). Since phenology parameters were jointly modified at all five sites, the optimized phenology parameters were the same at all sites in the synchrony optimization.

2.4. Experimental Design

[18] Given the two cost functions, and two forms of parameter optimization (asynchronous and synchronous), a total of three out of four experiments or model modes were analyzed here. These include asynchronous optimization with the equation (4) half-daily cost function ("A_H"), the asynchronous optimization with the equation (5) interannual cost function ("A_I"), and finally a synchronous optimization with the equation (5) cost function ("S"). Results from the fourth, synchronous optimization with the daily cost function, were performed but not discussed here since the results were nearly identical to the A_H experiment. The three experiments provide information about how well IAV can be parameterized and simulated at five sites by a simple ecosystem model (experiments A_H and A_I) as well as test how important synchronous phenological forcing drives coherent IAV (experiment S). Beyond comparing daily, seasonal, and cumulative NEE to observations, we also assess model parameters and compute carbon uptake period statistics. Carbon uptake period (C_{UP}) here was calculated as the start and end day of each year when 8 day smoothed daily observed or modeled NEE was negative (uptake).

3. Results

3.1. Seasonal Patterns

[19] Mean annual NEE at the five sites ranged from a large carbon sink (negative) to a moderate source (positive) of CO_2 to the atmosphere (Table 1). Mature forests such as US-WCr and US-UMB were the largest sinks followed by the shrub wetland (US-Los). In contrast, the old-growth forest (US-Syv) was near neutral (with large fluctuations between source and sink in any one year), and the mixed regional very tall tower (US-PFa) was the largest source. While the regional CO_2 source observed by the tower has been a continuing puzzle (see *Davis et al.* [2003] and *Ricciuto et al.* [2008] for further discussion and *Desai et al.* [2010] for a regional perspective), the other towers have NEE in line with expectations for vegetation type and latitude [*Yuan et al.*, 2009]. Uncertainty arising from random error, gap-filling and low-turbulence filtering was generally small and similar at all sites.

[20] Despite large variations in annual NEE, mean seasonal patterns at all five sites were quite similar (Figure 2, black line). Generally, sites started absorbing carbon in late May/early June, and crossed zero in cumulative NEE by mid-June, and turned back into carbon sources by late August or early September, except for US-PFa which turned into a carbon source much earlier in August. While the dates were similar for each site, small variations in those dates led to large differences in the length of observed C_{UP}, with the longest at the mature forests and wetlands, and shortest in the old-growth forest and regional site. This finding provides one basis that growing season timing and length were a strong controlling factor of annual carbon flux, and hence IAV.

[21] When compared to seasonal flux tower NEE, the IFUSE model (averaged across the same years as observations) generally replicated this pattern regardless of optimization mode (Figure 2, dotted and gray lines). In all cases, the A_H mode best replicated half-daily variations in NEE, explaining 83–93% of variability (Table 3), followed in most cases by A_I, except at US-UMB, where the S model outperformed A_I. Both A_H and A_I performed worst at US-PFa, perhaps because of the mixed footprint, while the S mode performed worst at US-Syv. All modes underestimated the strength of growing season uptake at US-PFa. Differences of model performance due to change in cost function are discussed in section 3.2. Visually (Figure 2), it is apparent that

Table 3. Percent of Variance Explained (r^2) and Mean Absolute Error of Observed NEE Anomalies Against the Model in Asynchronous Half-Daily Cost Function (A_H), Asynchronous Interannual Cost Function (A_I), and Synchronous (S) Experiments[a]

	Model	US-WCr	US-UMB	US-Syv	US-Los	US-PFa
Half-daily						
r^2	A_H	0.90	0.93	0.87	0.88	0.83
	A_I	0.81	0.82	0.84	0.85	0.77
	S	0.81	0.88	0.73	0.82	0.77
MAE	A_H	0.48	0.43	0.50	0.31	0.46
	A_I	0.78	0.59	0.53	0.37	0.55
	S	0.83	0.52	0.64	0.40	0.53
Interannual						
r^2	A_H	0.17	0.44	0.00	0.53	0.38
	A_I	0.87***	0.87**	0.69	0.76*	0.78**
	S	0.89***	0.64	0.24	0.88**	0.77**
MAE	A_H	109	28	95	12	39
	A_I	58	11	48	6	26
	S	46	31	71	9	25

[a]MAE, mean absolute error. All experiments were able to significantly capture daily variations NEE ($p < 0.01$), but A_I captured interannual variability at the most number of sites, followed by the S. All correlations at the half-daily scale were significant, while significance of model-data correlations of interannual variability are marked by *** ($p < 0.01$), ** ($p < 0.05$), and * ($p < 0.1$).

the A_I model better captured seasonal variation than A_H at most sites, especially at US-Syv, but for magnitude of annual NEE, all modes did well with respect to uncertainty in observations, except for A_H at US-Syv.

3.2. Interannual Variability

[22] IAV at all sites ranged from modest in the case of the wetland, to large in the case of the mature and old-growth forests (Table 1). When mean annual NEE over the entire time period is subtracted from observations of annual NEE and the anomalies are then normalized by dividing these values by one standard deviation of annual NEE, consistent patterns emerge among the sites (Figure 3). At most sites, IAV rarely exceeded σ, with the exception of 2001, coincident with a large regional forest tent caterpillar outbreak and particularly warm summer [*Cook et al.*, 2008]. Year-to-year fluctuations were quite common, and hints of a longer decadal-scale variability were evident. The spatial coherence of these anomalies is discussed in section 3.3.

[23] No relationship existed between NEE mean magnitude and σ IAV (Table 3). In absolute terms, IAV was smallest in the wetland, barely detectable within the uncertainty in mean NEE, and largest at US-WCr, the site most impacted by the 2001 insect outbreak. In the case of US-Syv, where mean NEE was near zero, the site trended from a sink in the first two years to a source in later years. In all cases, IAV was a major fraction of NEE.

[24] Despite all modes being able to capture most of the seasonal pattern of cumulative NEE at all sites, simulation of IAV anomalies was poor at all sites by A_H (Figure 4a), but significantly improved in A_I (Figure 4b). This result highlights the importance of the dual-likelihood cost function used by A_I. A_I IAV anomalies were significantly correlated ($p < 0.05$) to observed IAV anomalies at US-WCr, US-UMB, and US-PFa, strongly correlated ($p < 0.1$) to US-Los, and weakly correlated to US-Syv (Table 3). The trade-off, of course, was loss of explanation of variance at the half-daily scale ranging from 3 to 11% and an increase in mean absolute error of half-daily NEE by 0.03 to 0.3 gC m^{-2} d^{-1}.

[25] Further evidence that the fit of A_I to observations is not just an artifact of modeling comes when A_I L_{on} and L_{off} dates were compared to similar data observed at US-WCr (Figure 5). The observed dates were derived from calibrating a simple LAI model to the ratio of above and below canopy downwelling PAR and observed LAI [*Cook et al.*, 2008]. While correlations are modest, the model generally captured the pattern of anomalies in L_{ON} and L_{OFF}, though it did appear to underestimate the variability in L_{on} and overestimate the variability in L_{off}. The net effect, however, was good performance at simulating variations in growing season length.

[26] In parameter space, there are a number of differences between A_H (Table 4) and A_I (Table 5). Among phenology parameters, the net effect was in most but not all cases to increase the values of phenology slope parameters, α and β, consequently modifying the phenology climate thresholds. Covariances between these parameters and photosynthesis parameters then led to changes in LUE and temperature regulation of photosynthesis, since these parameters can also act like phenology parameters. Less clear were the reasons behind large changes in respiration parameters. While both A_H and A_I essentially optimized to a value of zero for b_3 (fraction of GPP respired), A_I has significantly smaller b_2 (less temperature sensitivity for plant growth respiration), and some large differences for b_1 for the mature forest sites, suggesting equifinality in model solutions for respiration and

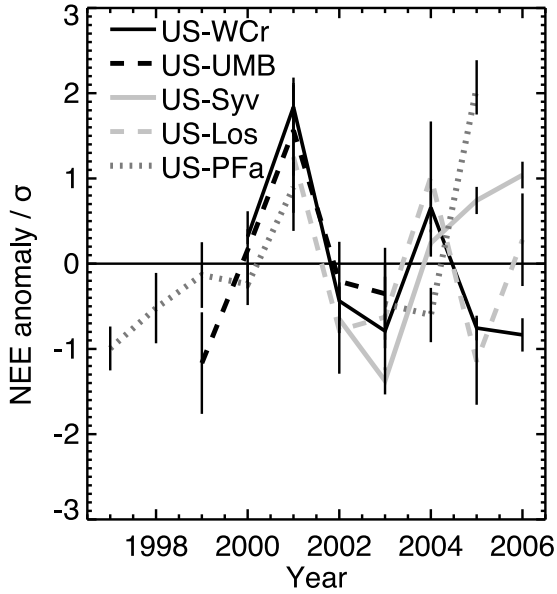

Figure 3. Observed standardized interannual variability in NEE (ratio of NEE anomaly to one standard deviation) at the five study sites. Strong coherence in variability in NEE was observed across the time period, even though absolute magnitudes in NEE variability varied widely. Observational uncertainty in NEE is noted by the horizontal bars.

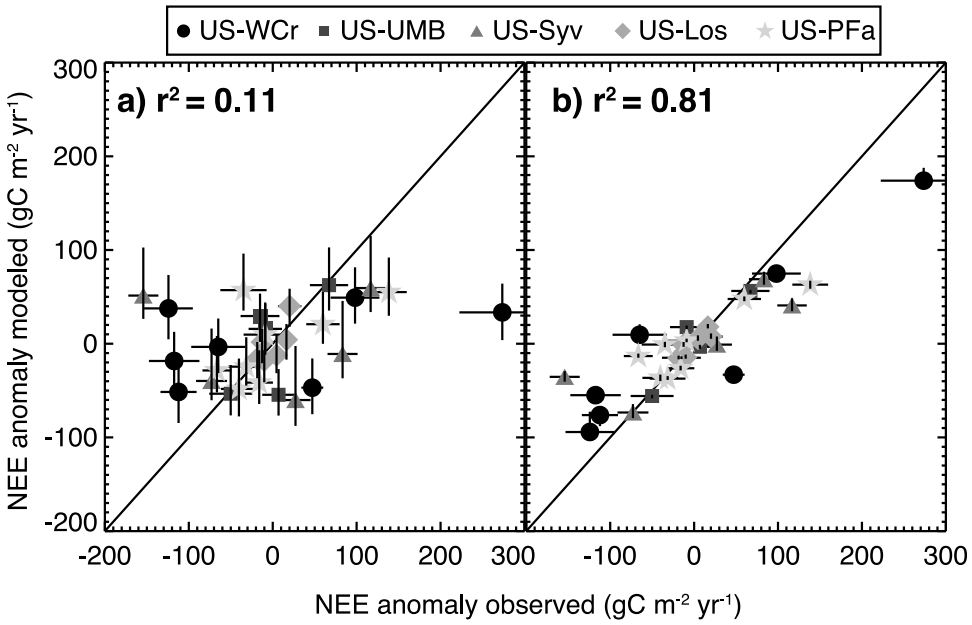

Figure 4. Correlation of anomalies in observed and modeled annual NEE using (a) the A_H cost function parameters (Table 4) and (b) the A_I cost function parameters (Table 5). Significant improvement in simulation of interannual variability was found for all sites in the latter.

highlighting the difficulty of estimating optimal respiration parameters from eddy covariance data.

3.3. Synchronous Forcing

[27] While the magnitude of NEE and IAV varied across sites and with time, coherent anomalies in IAV were readily observed when anomalies were statistically standardized (Figure 3). These results indicate the strong role that regional climate variability had on IAV. Even after taking NEE uncertainty into account, coherence was strong, with most sites showing positive anomalies in 2001 and 2004, and negative anomalies in 1999–2000, and 2002–2003. A bifurcation of trends across sites occurred in 2005 and 2006. While the tent caterpillar outbreak was one source of the anomaly in 2001, the outbreak was mostly felt at US-WCr in late spring, to a small extent in the US-PFa footprint, and barely at the other two sites, suggesting that climate anomalies still explained most of the 2001 NEE coherence.

[28] The S mode tested whether synchronous IAV can be explained by coupling of phenological parameters across sites. In this synchronous mode, the model still simulated much of the IAV at US-WCr, US-Los, and US-PFa ($p < 0.05$), but lost ability to simulate IAV at US-UMB, and like all modes, could not capture IAV at US-Syv (Table 3 and Figure 6). Correlation coefficients for the significant correlations were essentially unchanged compared to A_I. It is interesting to note that US-UMB is the further site from the rest (Figure 1), though it is equally likely that the decrease in IAV simulation skill may be related to differences in forest type compared to the other sites.

[29] The trade-off in half-daily NEE simulation for S compared to A_H was quite similar to the trade-off found for A_I, though with a larger drop in correlation at US-Syv. Across all sites, A_I has a strong correlation with observed IAV ($r^2 = 0.81$) (Figure 4b), but the S mode is still strongly correlated ($r^2 = 0.68$), and with 16 fewer parameters in aggregate compared to A_I. Photosynthesis and respiration parameters in A_I (Table 5) and S (Table 6) were more similar than between those and A_H (Table 4). Remarkably, the parameters in S appeared more in line with literature estimates than those for

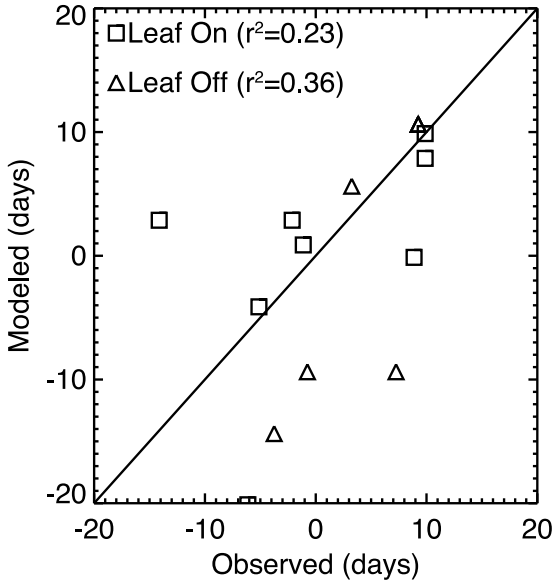

Figure 5. Comparison of observed light extinction profile derived leaf on (square) and leaf off (triangle) date anomalies to IFUSE model for the US-WCr site, using the A_I parameters. Generally, variability in both dates was modestly well simulated, though the slope of leaf off appears too steep, while the leaf on dates mostly fall on the 1:1 line except for one outlier.

Table 4. Best and Range of Accepted Posterior Model Parameters for Each Site Using the Asynchronous Half-Daily Cost Function (A_H)

Name	US-WCr	US-UMB	US-Syv	US-Los	US-PFa
			Phenology Parameters		
A	0.089 (0.085–0.094)	0.142 (0.122–0.156)	0.195 (0.154–0.283)	0.206 (0.186–0.219)	0.160 (0.130–0.185)
GDD_{thresh}	154.0 (153.8–156.1)	107.1 (102.1–111.3)	81.1 (77.3–84.9)	80.7 (79.9–80.8)	131.5 (131.2–131.6)
B	0.182 (0.155–0.200)	0.165 (0.138–0.198)	0.098 (0.074–0.147)	0.091 (0.070–0.108)	0.135 (0.082–0.199)
$TEMP_{thresh}$	11.3 (11.1–11.8)	9.0 (8.9–9.2)	9.6 (9.2–11.1)	11.4 (11.3–11.4)	10.2 (9.2–10.9)
			Photosynthesis Parameters		
LUE	0.273 (0.262–0.281)	0.441 (0.326–0.444)	0.286 (0.265–0.371)	0.195 (0.187–0.251)	0.193 (0.179–0.200)
T_{min}	−5.6 (−15.0–1.7)	−15.0 (−15.0–14.2)	−14.0 (−15.0–10.7)	−11.0 (−14.9–7.1)	−3.5 (−7.7–0.4)
T_{opt}	6.7 (5.0–9.2)	39.1 (27.1–40.0)	29.5 (27.2–40.0)	32.1 (29.7–40.0)	11.0 (7.9–12.8)
VPD_{max}	4125 (3797–4562)	3143 (3016–3292)	3565 (3291–3908)	3893 (3636–4344)	3571 (3223–3929)
VPD_{min}	2 (0–115)	73 (0–309)	18 (0–235)	421 (15–513)	0 (0–201)
			Respiration Parameters		
r_s	1.01 (0.76–1.17)	0.11 (0.10–0.25)	0.12 (0.10–0.37)	0.55 (0.40–0.70)	0.73 (0.51–0.99)
r_v	0.22 (0.11–0.45)	0.95 (0.83–1.00)	1.55 (1.32–1.68)	0.65 (0.53–0.74)	0.71 (0.54–0.90)
b_1	0.0954 (0.0763–0.1238)	0.3812 (0.2634–0.4216)	0.1595 (0.0204–0.3538)	0.1091 (0.0923–0.1343)	0.1111 (0.0840–0.1405)
b_2	0.0275 (0.0002–0.0806)	0.0438 (0.0349–0.0499)	0.0811 (0.0730–0.0927)	0.0879 (0.0757–0.0983)	0.0872 (0.0723–0.1066)
b_3	0.0001 (0–0.0052)	0.0007 (0–0.0112)	0.0001 (0–0.0391)	0.0121 (0.0001–0.0299)	0.0995 (0.0655–0.1221)

A_I, especially T_{opt}. Phenology parameters in S are fixed for all five sites, and appeared to fall roughly near the average of those parameters for each site in A_I.

4. Discussion

4.1. Modeling of IAV

[30] The observed IAV is within the range (~50–100 gC m^{-2} yr^{-1}) observed for deciduous broadleaf forests in midlatitudes [*Yuan et al.*, 2009], with mature northern hardwood forests exhibiting the largest. The results here contribute to findings of interannual variations in seasonal temperature as a dominant driving force of interannual variation in carbon flux at midlatitudes [*Sierra et al.*, 2009; *Yuan et al.*, 2009]. While these sites only had 5–8 years of data, typical of most flux tower sites, the analysis here showed that information about IAV can still be gleaned by combining all sites in a similar region, and jointly parameterizing a model with multiple years of data at each site and evaluating across longer sets. Certainly, longer data to estimate lower frequency trends in flux tower data are critical. This analysis also suggests that extending flux tower records with phenological indicators of growing season length and carbon uptake period, perhaps through remote sensing, would be one way forward to better assess the links between climate variability and carbon cycle impacts.

[31] Given the observed coherent IAV across space and likelihood that seasonal temperature fluctuations were important in the study region, it is not entirely surprising that a model tuned to capture daily to seasonal climate sensitivity of carbon cycling can adequately capture the observed IAV, especially given that seasonal climate forcing strongly influenced modeled ecosystem growing season length and timing. Rather, what is surprising is the level of care needed for proper parameterization and the importance of not just identifying optimal model structure and parameters, but also optimal model cost functions. In this case, as in many ecosystem models, the failure of a simple MCMC approach in tuning parameters for simulating IAV relies partly on the large signal imparted by CO_2 flux diurnal variability (large

Table 5. Same as Table 4 but for the Asynchronous Interannual Cost Function (A_I)

Name	US-WCr	US-UMB	US-Syv	US-Los	US-PFa
			Phenology Parameters		
A	0.093 (0.084–0.097)	0.500 (0.467–0.500)	0.130 (0.113–0.139)	0.249 (0.245–0.251)	0.050 (0.050–0.051)
GDD_{thresh}	130.2 (127.6–130.3)	71.5 (71.4–71.5)	56.4 (56.3–56.9)	58.2 (57.1–58.4)	149.6 (149.4–149.8)
B	0.490 (0.317–0.500)	0.050 (0.050–0.053)	0.051 (0.050–0.059)	0.476 (0.450–0.483)	0.050 (0.050–0.050)
$TEMP_{thresh}$	1.4 (1.4–1.4)	−7.4 (−8.0–6.8)	14.6 (14.5–14.7)	8.3 (8.1–8.5)	−5.6 (−6.9–5.1)
			Photosynthesis Parameters		
LUE	0.463 (0.444–0.483)	0.204 (0.202–0.205)	0.244 (0.231–0.250)	0.183 (0.179–0.188)	0.159 (0.156–0.162)
T_{min}	−0.2 (−0.3–0.2)	8.9 (8.8–9.0)	6.7 (6.7–6.8)	−4.1 (−4.1–4.0)	5.0 (5.0–5.0)
T_{opt}	36.3 (34.6–37.8)	19.6 (19.5–19.7)	7.0 (6.9–7.0)	30.7 (30.3–31.5)	5.1 (5.1–5.2)
VPD_{max}	19802 (15935–19998)	2230 (2184–2301)	3681 (3489–3930)	4074 (3874–4314)	13304 (2110–19973)
VPD_{min}	10 (0–239)	1536 (1506–1549)	3 (0–209)	542 (480–603)	1964 (1732–1999)
			Respiration Parameters		
r_s	0.23 (0.22–0.24)	0.81 (0.78–0.81)	1.29 (1.21–1.41)	0.31 (0.28–0.33)	0.59 (0.55–0.63)
r_v	1.06 (1.04–1.12)	0.10 (0.10–0.12)	0.97 (0.86–1.05)	0.89 (0.86–0.92)	1.43 (1.39–1.47)
b_1	0.4999 (0.4979–0.5000)	0.0449 (0.0414–0.0449)	0.1395 (0.1330–0.1461)	0.1859 (0.1729–0.2043)	0.0897 (0.0824–0.0944)
b_2	0.0001 (0–0.0011)	0.0002 (0–0.0184)	0.0001 (0–0.0020)	0.0769 (0.0745–0.0797)	0.0836 (0.0798–0.0883)
b_3	0 (0–0.0010)	0.0005 (0–0.0044)	0.0002 (0–0.0066)	0.0004 (0–0.0058)	0 (0–0.0016)

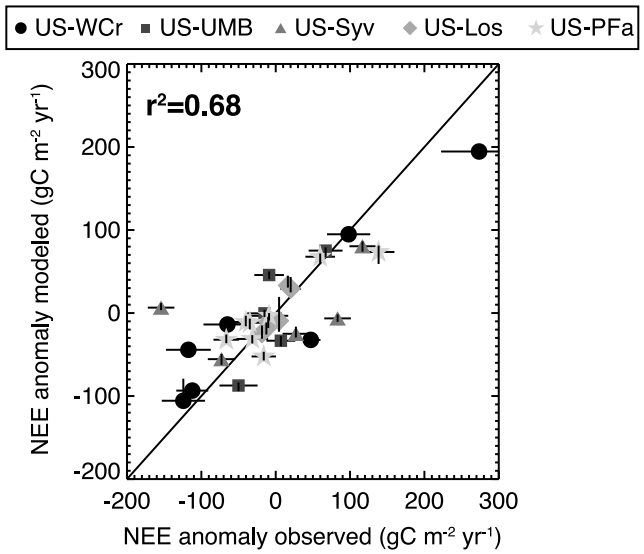

Figure 6. Same as Figure 4 but for the S cost function parameters (Table 6). Interannual variations by the S model were well simulated for most sites, but less successfully for US-UMB and quite poorly for US-Syv.

and negative in day, large and positive at night), which tends to mask the more subtle, but perhaps more climatically relevant, interannual signal [*Stoy et al.*, 2009].

[32] The simulation presented here, consequently, is one of few models that has been able to successfully diagnose interannual variability of NEE within a relatively simple ecosystem model. Other well-known, and arguably more sophisticated models have shown less ability to model IAV in north temperate forested regions [*Ricciuto et al.*, 2008; *Urbanski et al.*, 2007]. It is likely, at least in the case of the northeastern forest studied by *Urbanski et al.* [2007], that successional trajectory was an important factor in long-term variability at the site, possibly overwhelming a climate variability signal. A major shortcoming of the approach used here is the inability to estimate how important succession and disturbance is part of subdecadal IAV. Investigations at decadal or longer timescales would certainly need to incorporate these processes. Further, the steady state spin-up assumption made by developing a model with no carbon pools would not be valid, and other techniques should be implemented with a pool based model [e.g., *Carvalhais et al.*, 2008].

[33] Analysis also revealed large variation in IAV variance explained by this model within a small region that appeared to vary as a function of vegetation type, highlighting the importance of individual site characteristics in determining the extent to which interannual carbon cycling may be more controlled by climate or internal biotic dynamics [*Polley et al.*, 2010]. Strong internal control of NEE variability appears to have played a part in the lack of model predictive ability at the old-growth forest. *Desai et al.* [2005] also highlighted the greater sensitivity to moisture stress that has been found at this forest compared to nearby mature forests.

[34] One way to assess biotic control that has been demonstrated both by *Polley et al.* [2010] and *Richardson et al.* [2007] is to compare model parameterization with fixed parameters over multiple years against interannually varying parameters, the latter reflecting variability in biotic controls on NEE. *Polley et al.* [2010] argued that biotic control of interannual variability was significant in grasslands, and *Richardson et al.* [2007] similarly argued that the majority (55%) of interannual variations in a spruce forest in the northeast United States was driven by biotic variation. Though this study did not test a model with variable parameters, the findings here of strong explanation by a simple model with fixed-in-time parameters suggests that, at least for mature hardwood forests of boreal-temperate transition reasons, climate sensitivity, especially of spring and fall, drove interannual variation of NEE.

[35] While the model was able to simulate IAV at the wetland, it was more designed with forest productivity and aerobic decomposition in mind, suggesting nonshrub or precipitation-fed wetlands would not fare as well as the shrub fen studied here. Still, this particular wetland site was not in steady state over the time period due to a significant ongoing decline in water table [*Sulman et al.*, 2009]. *Sulman et al.* [2009] showed that water table influences both respiration

Table 6. Same as Table 4, but for the Synchronous Cost Function (S)

Name	US-WCr	US-UMB	US-Syv	US-Los	US-PFa
			Phenology Parameters (Jointly Optimized)		
A	0.063 (0.061–0.065)				
GDD_{thresh}	165.3 (165.2–165.3)				
B	0.100 (0.084–0.112)				
$TEMP_{thresh}$	4.8 (4.7–4.8)				
			Photosynthesis Parameters		
LUE	0.299 (0.295–0.305)	0.495 (0.479–0.520)	0.300 (0.289–0.310)	0.260 (0.251–0.276)	0.159 (0.154–0.162)
T_{min}	4.0 (4.0–4.0)	−2.8 (−3.0–2.0)	9.4 (9.4–9.5)	2.7 (2.7–3.0)	−4.0 (−4.7–3.9)
T_{opt}	21.3 (21.0–21.6)	38.1 (36.9–39.9)	21.2 (21.0–21.8)	37.8 (36.4–40.0)	20.5 (19.4–21.2)
VPD_{max}	11931 (2010–19999)	3399 (3279–3647)	3389 (3261–3530)	4028 (3339–4565)	11206 (2442–19991)
VPD_{min}	1981 (1647–1999)	287 (99–369)	144 (10–229)	760 (721–956)	1943 (1084–1999)
			Respiration Parameters		
r_s	0.23 (0.22–0.24)	0.90 (0.81–0.92)	1.79 (1.74–1.81)	0.31 (0.28–0.52)	0.35 (0.26–0.45)
r_v	1.26 (1.23–1.29)	0.34 (0.30–0.39)	0.10 (0.10–0.12)	0.91 (0.71–0.93)	1.31 (1.26–1.37)
b_1	0.4999 (0.4984–0.5000)	0.1073 (0.0987–0.1165)	0.2103 (0.2032–0.2146)	0.2720 (0.1780–0.3230)	0.2689 (0.2058–0.3217)
b_2	0 (0–0.0009)	0.0002 (0.0000–0.0058)	0.0014 (0.0000–0.0187)	0.0859 (0.0635–0.0885)	0.0932 (0.0867–0.0991)
b_3	0 (0–0.0005)	0.0003 (0–0.0050)	0 (0–0.0035)	0.0004 (0–0.0245)	0.0014 (0–0.0142)

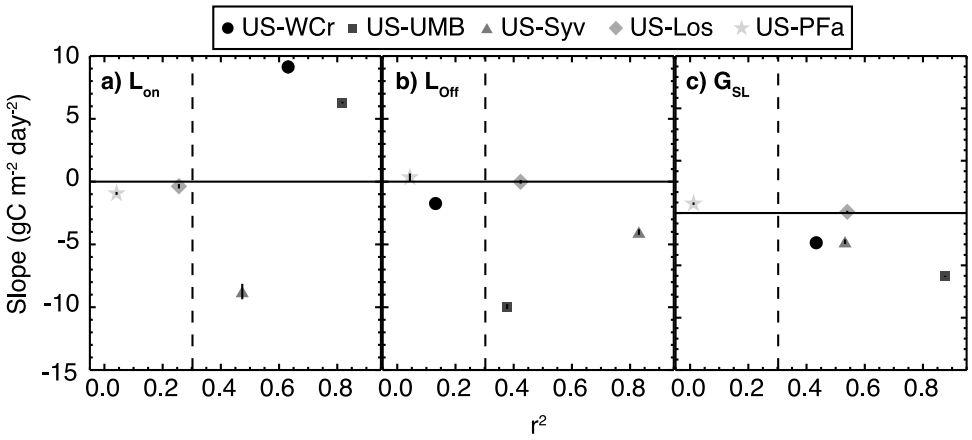

Figure 7. Linear regression derived slope of the relationship between annual NEE and anomaly in dates of (a) leaf on (L_{ON}), (b) leaf off (L_{OFF}), and (c) growing season length (G_{SL}) as quantified from IFUSE model output using A_I cost function parameters (Table 5) plotted against linear correlation of this relationship at all sites. Dotted line indicates $p < 0.1$ significance level.

and productivity in this wetland, generally leading to little change in NEE over the time period studied. Consequently, one could argue that this model may be getting the right answer for the wrong reasons, given the relatively small interannual variability of NEE.

[36] Differing model structures led the MCMC algorithm to select different optimal values for many parameters. When the models were compared in parameter space, it was not always immediately obvious how other parameter differences between the models improved the fit to IAV. These parameter correlations require further examination and suggest that caution is required when drawing inferences from model parameter optimization techniques without first testing for optimal model structure. Additionally, a question of overfitting to IAV arises when relying on data sets with only a few years of data and the modified cost function, which also requires further examination.

4.2. Synchronous Phenological Forcing

[37] Surprisingly, despite the differences in site ecosystem type, age, and location, the simulation with synchronous phenological forcing still managed to explain much of the IAV in the region, especially for forests. Though the details of plant phenology vary strongly by species and the microclimate experienced by individual plants, results here suggest that at stand or regional scale, carbon cycle responses to climate can generally be simulated by relatively simple accumulated climatic heating indices and regional soil temperature thresholds. Within this framework, it would make sense that US-UMB would fare poorest under synchronous forcing, as it is the farthest site both climatically and geographically from the other sites, while the other four sites are more similar in climate and soil type. However, this assertion cannot be rigorously tested here without also comparing to forest similar to US-UMB at varying distances. Still, these results hint at a possible way to better estimate the spatial coherence of phenological forcing by utilizing sets of flux towers to geostatistically test the ability of models to jointly simulate flux variability [*Yadav et al.*, 2010]. Here, the findings suggest synchronous scales of at least 100 km, reflecting the distance among the tower sites outside of US-UMB. Also, the decline in explanation of variance at the old growth forest further develops the case that this site has strong internal control on interannual carbon cycling.

4.3. Carbon Cycling and Growing Season Length

[38] The parameterized A_I model can be further examined to suggest mechanisms by which climate variability is connected to flux variability, via the interaction of model parameters that impact growing season length (Figure 7) and carbon uptake period (Figure 8). For sites where the A_I model successfully simulated IAV, the mechanism by which phenology impacted IAV was not consistent across all sites. Hardwood forest sites (US-WCr and US-UMB) showed less carbon uptake (more positive NEE) with later L_{ON}, while other sites had no significant relationship (Figure 7a). For these two sites, the strength of this L_{ON} relationship drove a negative relationship between growing season length (G_{SL}) and NEE (longer G_{SL} = more uptake). This finding is consistent with previous single site studies that have noted relationships between warmer springs and enhanced annual carbon uptake in a boreal aspen forest [*Barr et al.*, 2006; *Chen et al.*, 1999], eastern deciduous forest [*Goulden et al.*, 1996], and a spruce-dominated eastern forest [*Hollinger et al.*, 2004; *Richardson et al.*, 2009].

[39] The effect of autumn (L_{OFF}) is less clear, with one only forest (US-Syv) showing a significant positive relationship (later L_{OFF} = less uptake) (Figure 7b). The wetland site (US-Los) also had a significant relationship, but the magnitude was very small. A recent paper noted that warmer autumns led to less carbon uptake in boreal ecosystems, by increasing ER more than GPP [*Piao et al.*, 2008]. This effect is not strongly evident here in the temperate-boreal transition zone.

[40] While strong consistent spring and autumn climate impacts on NEE were not apparent, the combined effect of both on G_{SL} is significant and negative (longer growing season is equal to more carbon uptake) at all sites except the mixed regional site (US-PFa), consistent with earlier findings across the flux tower network showing growing season length as a strong determinant of net carbon uptake [*Baldocchi et al.*, 2001; *Churkina et al.*, 2005]. The lack of strong correlation at the US-PFa site may be related to complementary responses

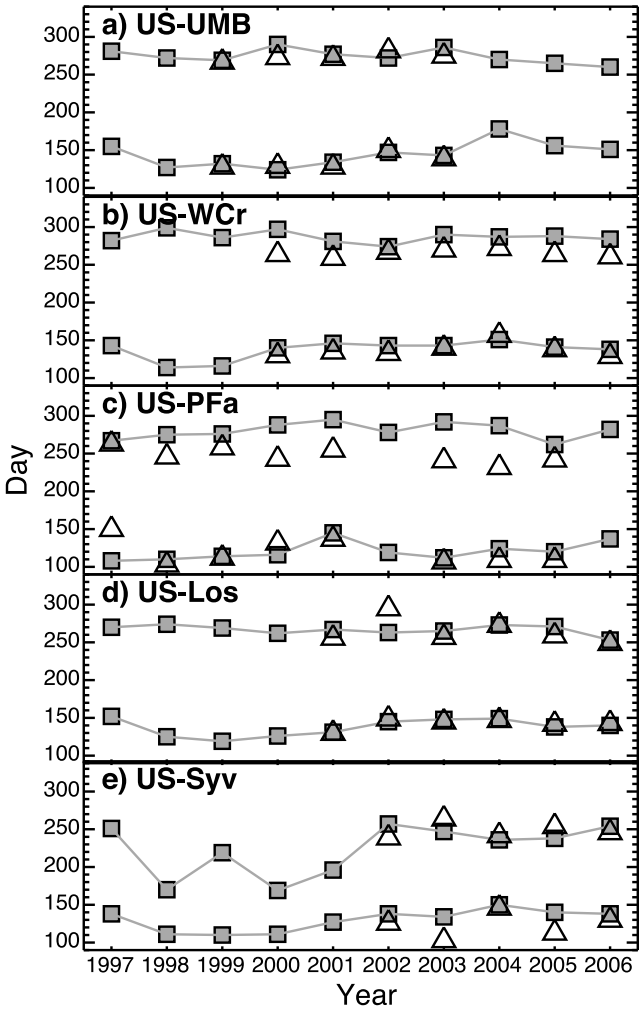

Figure 8. Comparison of model (solid square, line) and observed (open triangle) carbon uptake start and end dates for each year at each site sorted by latitude (south to north). Observed and modeled dates match well, though US-PFa end dates were overestimated by model, and US-Syl showed large variability in the first several years. No strong latitudinal trends were detected in start date, but a linear trend was found of earlier end dates with greater latitude.

occurring across the mix of stand types sampled by the tall tower and perhaps the influence of moisture on regional fluxes that is not apparent at the stand-scale towers [*Desai et al.*, 2010].

[41] Interestingly, while the parameter analysis suggests that spring phenology was a strong controller of growing season length for mature forests, analysis of C_{UP} showed mean variability in end date of C_{UP} (+/− 13 days) was virtually the same as start date (+/− 14 days) at most sites (Figure 8), though some of this was driven by significant variability in C_{UP} end date simulated at the old growth site. The simulated C_{UP} was relatively well matched to observed variation in C_{UP}, except for overestimate of C_{UP} end date at US-PFa, most likely related to the complex footprint observed at this site. Spatially, C_{UP} ends dates were more variable across sites (+/− 25 days) than start dates (+/− 9 days), and the former had a negative latitudinal trend (earlier end date further north), while the latter had no discernible trend. Rather, it appears the earliest C_{UP} dates were associated with sites that have more evergreen trees in the footprint (US-PFa and US-Syl), and the date of net carbon uptake start otherwise is strongly spatially coherent, whereas end date is more site-dependent, with the latitudinal trend probably spurious given the variation in ecosystem type. Further analysis of climatic controls revealed that the C_{UP} start dates were strongly correlated to mean annual temperature at the mature and old-growth forest sites (r^2 ranging from 0.50 to 0.87), while end dates had no significant relationships to temperature or radiation. C_{UP} start was also well correlated to mean annual incoming PAR, but the climate data showed a strong relationship between mean annual PAR and temperature ($r = -0.82$). These findings highlight aspects of climatic spatial coherence and possible remote sensing approaches to quantifying regional carbon uptake periods and phenology.

[42] There is also evidence to suggest that relationships between water and carbon cycle, something not modeled here, are an important factor to consider when simulating carbon cycle IAV. *Hu et al.* [2010] found that evergreen montaine forest carbon uptake had an inverse relationship with growing season length, due to the importance of snowmelt as a source of growing season plant available water. The findings here, showing mostly the opposite case, do not suggest a strong control of snow water on IAV in the study region. However, other studies in the region have shown that water table depth [*Desai et al.*, 2010; *Sulman et al.*, 2009] and summer soil moisture [*Ricciuto et al.*, 2008] may also be important factors in explaining IAV in the patchy forest-wetland landscape that characterizes the region, and in similar forests of other regions [*Hollinger et al.*, 2004]. *Ricciuto et al.* [2008] noted that daytime and seasonal NEE at the regional tall tower (US-PFa) were correlated to soil moisture, but correlations were weak at the annual scale. The models used here did not consider these effects, which may explain some of the unexplained variability of IAV, especially at the wetland and old-growth forest. Time lags are likely in relationships between moisture and carbon [e.g., *Desai et al.*, 2010; *Dunn et al.*, 2007; *Hu et al.*, 2010], and model mechanisms to couple these processes require further assessment.

5. Conclusion

[43] Thirty-one site years of near continuous flux tower carbon exchange observations across a meso-network of five established Ameriflux sites were used to identify a coherent signal of interannual variability in net ecosystem exchange, a likely indicator of the role of regional climate variability on ecosystem carbon cycling. A model parameterized with climate-sensitive phenology and a minimal set of carbon cycle functions and parameters to explain daily variations in NEE could successfully simulate much of this IAV, especially at the mature forest sites, but only when the model cost function was correctly identified and applied.

[44] Climate variability in this boreal-temperate transition region drove NEE variability in the model primarily through the impact of growing season length on length of carbon uptake period. Given the longer timescales over which decomposition and respiration processes vary (i.e., slowly varying soil pools), it was not surprising that most interannual variability in these sites can be ascribed to photosynthetic

processes. The model also highlighted the role that climate variability imparts on carbon flux spatial coherence, at least on length scales of 100 km for this region, though this question would be best further explored with a larger-scale geostatistical study of carbon flux spatial variation [*Yadav et al.*, 2010].

[45] Old-growth forest and wetland annual carbon flux variability were less well simulated, suggesting a strong role for internal biotic dynamics and moisture variability on carbon flux variations at some sites. These dynamics may be an important aspect of regional carbon cycle variability, especially as forests in the region age and long-term drought conditions persist. Other noted causes of IAV that also require further consideration, especially at regional scales, include the role of stochastic disturbance [*Desai et al.*, 2007], pest outbreaks [*Cook et al.*, 2008], and internal organic matter decomposition dynamics [*Ricciuto et al.*, 2008].

[46] These findings highlight the complexities involved in upscaling flux tower NEE and simulating regional carbon fluxes with ecosystem models. While some level of common responses of climate variability and carbon uptake can be specified, as shown here, it is obvious that not all subgrid variability (i.e., for example in this region, the role of stand age and wetlands) can be sufficiently simulated with this kind of approach. Depending on the extent of subgrid variability within any one region and the research questions being asked, it is recommended that ecosystem modelers further investigate how to best specify and parameterize this variability in regional- and global-scale models.

[47] The impact of climate variability on phenology and ultimately ecosystem biogeochemistry is a first-order climate-ecosystem interaction, and of likely importance on the predictability of future carbon cycles as anthropogenic climatic changes are expected to be strongly felt in midcontinental midlatitude regions. Preliminary findings from long-term flux tower observations and careful ecosystem model parameterization in a boreal-temperate transition region suggest that future climate change in the shoulder seasons is likely to affect the carbon balance of mixed and deciduous broadleaf forests, perhaps more than climatic changes occurring in the central part of the growing season. However, these findings are limited by lack of longer-term carbon cycle and phenological observations. Additionally, the variety of findings among montaine, grassland, temperate, boreal, and temperate-boreal transition regions highlight the need for continued efforts to better parameterize climate sensitivity of phenology in ecosystem models.

[48] **Acknowledgments.** Flux tower observations could not have been made without the assistance of those associated with the Chequamagon Ecosystem-Atmosphere Study (ChEAS), especially K. Davis of Pennsylvania State University, J. Thom and S. Knuth of University of Wisconsin-Madison, B. Cook of NASA Goddard Space Flight Center, D. Ricciuto of Oak Ridge National Labs, P. Curtis of Ohio State University, C. Gough of Virginia Commonwealth University, C. Vogel of University of Michigan Biological Station, R. Teclaw and D. Baumann of the US Forest Service Northern Research Station, and R. Strand of the Wisconsin Education Communications Board (ECB). I also would like to thank B. Sacks, University of Wisconsin-Madison, for discussion of parameter estimation techniques and the Center for Climatic Research (CCR) for support. This work was supported by the Department of Energy (DOE) Office of Biological and Environmental Research (BER) National Institute for Climatic Change Research (NICCR) Midwestern Region Subagreement 050516Z19 and the National Science Foundation (NSF) Biology Directorate grant DEB-0845166.

References

Baldocchi, D. D., et al. (2001), FLUXNET: A new tool to study the temporal and spatial variability of ecosystem-scale carbon dioxide, water vapor, and energy flux densities, *Bull. Am. Meteorol. Soc.*, *82*, 2415–2434.

Baldocchi, D. D., et al. (2005), Predicting the onset of net carbon uptake by deciduous forests with soil temperature and climate data: A synthesis of FLUXNET data, *Int. J. Biometeorol.*, *49*, 377–387.

Barr, A. G., et al. (2006), Climatic controls on the carbon and water balances of a boreal aspen forest, 1994–2003, *Global Change Biol.*, *13*, 561–576.

Bonan, G. B. (2008), Forests and climate change: Forcings, feedbacks, and the climate benefits of forests, *Science*, *320*(5882), 1444–1449, doi:10.1126/science.1155121.

Braswell, B. H., B. Sacks, E. Linder, and D. S. Schimel (2005), Estimating ecosystem process parameters by assimilation of eddy flux observations of NEE, *Global Change Biol.*, *11*, 335–355.

Carvalhais, N., et al. (2008), Implications of the carbon cycle steady state assumption for biogeochemical modeling performance and inverse parameter retrieval, *Global Biogeochem. Cycles*, *22*, GB2007, doi:10.1029/2007GB003033.

Chen, W. J., et al. (1999), Effects of climatic variability on the annual carbon sequestration by a boreal aspen forest, *Global Change Biol.*, *5*, 41–53.

Churkina, G., D. Schimel, B. H. Braswell, and X. M. Xiao (2005), Spatial analysis of growing season length control on net ecosystem exchange, *Global Change Biol.*, *11*, 1777–1787.

Cook, B. D., et al. (2004), Carbon exchange and venting anomalies in an upland deciduous forest in northern Wisconsin, USA, *Agric. For. Meteorol.*, *126*, 271–295.

Cook, B. D., P. V. Bolstad, J. G. Martin, F. A. Heinsch, K. J. Davis, W. Wang, A. R. Desai, and R. M. Teclaw (2008), Using light-use and production efficiency models to predict forest production and carbon exchange during canopy disturbance events, *Ecosystems*, *11*, 26–44, doi:10.1007/s10021-007-9105-0.

Davis, K. J., et al. (2003), The annual cycle of CO_2 and H_2O exchange over a northern mixed forest as observed from a very tall tower, *Global Change Biol.*, *9*, 1278–1293.

Desai, A. R., P. V. Bolstad, B. D. Cook, K. J. Davis, and E. V. Carey (2005), Comparing net ecosystem exchange of carbon dioxide between an old-growth and mature forest in the upper Midwest, USA, *Agric. For. Meteorol.*, *128*(1–2), 33–55, doi:10.1016/j.agformet.2004.09.005.

Desai, A. R., P. R. Moorcroft, P. V. Bolstad, and K. J. Davis (2007), Regional carbon fluxes from a biometrically constrained dynamic ecosystem model: Impact of disturbance, CO_2 fertilization and heterogeneous land cover, *J. Geophys. Res.*, *112*, G01017, doi:10.1029/2006JG000264.

Desai, A. R., et al. (2008), Influence of vegetation and seasonal forcing on carbon dioxide fluxes across the Upper Midwest, USA: Implications for regional scaling, *Agric. For. Meteorol.*, *148*(2), 288–308, doi:10.1016/j.agrformet.2007.08.001.

Desai, A. R., B. R. Helliker, P. R. Moorcroft, A. E. Andrews, and J. A. Berry (2010), Climatic controls of interannual variability in regional carbon fluxes from top-down and bottom-up perspectives, *J. Geophys. Res.*, *115*, G02011, doi:10.1029/2009JG001122.

Dragoni, D., H. P. Schmid, C. A. Wayson, H. Potter, C. S. B. Grimmond, and J. Randolph (2010), Evidence of increased net ecosystem productivity associated with a longer vegetated season in a deciduous forest in south-central Indiana, USA, *Global Change Biol.*, doi:10.1111/j.1365-2486.2010.02281.x, in press.

Dunn, A. L., C. C. Barford, S. C. Wofsy, M. L. Goulden, and B. C. Daube (2007), A long-term record of carbon exchange in a boreal blackspruce forest: Means, responses to interannual variability, and decadal trends, *Global Change Biol.*, *13*, 577–590.

Gordo, O., and J. J. Sanz (2010), Impact of climate change on plant phenology in Mediterranean ecosystems, *Global Change Biol.*, *16*, 1082–1106, doi:10.1111/j.1365-2486.2009.02084.x.

Gough, C. M., C. S. Vogel, H.-P. Schmid, H.-B. Su, and P. S. Curtis (2008), Multi-year convergence of biometric and meteorological estimates of forest carbon storage, *Agric. For. Meteorol.*, *148*, 158–170.

Goulden, M. L., J. W. Munger, S. M. Fan, B. C. Daube, and S. C. Wofsy (1996), Exchange of carbon dioxide by a deciduous forest: Response to interannual climate variability, *Science*, *271*, 1576–1578.

Hollinger, D. Y., J. Aber, B. Dail, S. M. Davidson, H. Goltz, and H. Hughes (2004), Spatial and temporal variability in forest-atmosphere CO_2 exchange, *Global Change Biol.*, *10*, 1689–1706.

Hu, J., D. J. P. Moore, S. P. Burns, and R. K. Monson (2010), Longer growing seasons lead to less carbon sequestration by a subalpine forest, *Global Change Biol.*, *16*, 771–783, doi:10.1111/j.1365-2486.2009.01967.x.

Linderholm, H. W. (2006), Growing season changes in the last century, *Agric. For. Meteorol.*, *137*, 1–14.

Luo, Y. Q., E. S. Weng, X. W. Wu, C. Gao, X. H. Zhou, and L. Zhang (2009), Parameter identifiability, constraint, and equifinality in data assimilation with ecosystem models, *Ecol. Appl.*, *19*, 571–574.

Menzel, A., and P. Fabian (1999), Growing season extended in Europe, *Nature*, *455*, 213–215.

Metropolis, N., and S. Ulam (1949), The Monte Carlo method, *J. Am. Stat. Assoc.*, *44*, 335–341.

Moffat, A. M., et al. (2007), Comprehensive comparison of gap filling techniques for eddy covariance net carbon fluxes, *Agric. For. Meteorol.*, *147*, 209–232.

Morisette, J. T., et al. (2009), Tracking the rhythm of the seasons in the face of global change: Phenological research in the 21st century, *Front. Ecol. Environ*, *7*, 253–260, doi:10.1890/070217.

Myneni, R. B., C. D. Keeling, C. J. Tucker, G. Asrar, and R. R. Nemani (1997), Increasing plant growth in the northern high latitudes from 1981 to 1991, *Nature*, *386*, 698–702.

Peñuelas, J., T. Rutishauser, and I. Filella (2009), Phenology feedbacks on climate change, *Science*, *324*(5929), 887–888, doi:10.1126/science.1173004.

Piao, S., et al. (2008), Net carbon dioxide losses of northern ecosystems in response to autumn warming, *Nature*, *451*, 49–53.

Polley, H. W., et al. (2010), Physiological and environmental regulation of interannual variability in CO_2 exchange on rangelands in the western United States, *Global Change Biol.*, *16*, 990–1002, doi:10.1111/j.1365-2486.2009.01966.x.

Ricciuto, D. M., M. P. Butler, K. J. Davis, B. D. Cook, P. S. Bakwin, A. Andrews, and R. M. Teclaw (2008), Causes of interannual variability in ecosystem-atmosphere CO_2 exchange in a northern Wisconsin forest using a Bayesian model calibration, *Agric. For. Meteorol.*, *148*(2), 309–327.

Richardson, A. D., A. S. Bailey, E. G. Denny, C. W. Martin, and J. O'Keefe (2006), Phenology of a northern hardwood forest canopy, *Global Change Biol.*, *12*, 1174–1178.

Richardson, A. D., D. Y. Hollinger, J. D. Aber, S. V. Ollinger, and B. H. Braswell (2007), Environmental variation is directly responsible for short- but not long-term variation in forest-atmosphere carbon exchange, *Global Change Biol.*, *13*, 788–803.

Richardson, A. D., D. Y. Hollinger, D. B. Dail, J. T. Lee, J. W. Munger, and J. O'Keefe (2009), Influence of spring phenology on seasonal and annual carbon balance in two contrasting New England forests, *Tree Physiol.*, *29*, 321–331, doi:10.1093/treephys/tpn040.

Sacks, W. J., D. S. Schimel, R. K. Monson, and B. H. Braswell (2006), Model-data synthesis of diurnal and seasonal CO_2 fluxes at Niwot Ridge, Colorado, *Global Change Biol.*, *12*(2), 240–259.

Sierra, C., H. W. Loescher, M. E. Harmon, A. D. Richardson, D. Y. Hollinger, and S. S. Perakis (2009), Interannual variation of carbon fluxes from three contrasting evergreen forests: The role of forest dynamics and climate, *Ecology*, *90*(10), 2711–2723.

Stine, A. R., P. Huybers, and I. Y. Fung (2009), Changes in the phase of the annual cycle of surface temperature, *Nature*, *457*, 435–441, doi:10.1038/nature07675.

Stöckli, R., and P. L. Vidale (2004), European plant phenology and climate as seen in a 20-year AVHRR land-surface parameter dataset, *Int. J. Remote Sens.*, *25*, 3303–3330.

Stoy, P. C., et al. (2009), Biosphere-atmosphere exchange of CO_2 in relation to climate: A cross-biome analysis across multiple time scales, *Biogeosciences*, *6*, 2297–2312.

Sulman, B. N., A. R. Desai, B. D. Cook, N. Saliendra, and D. S. Mackay (2009), Contrasting carbon dioxide fluxes between a drying shrub wetland in northern Wisconsin, USA, and nearby forests, *Biogeosciences*, *6*, 1115–1126.

Urbanski, S., et al. (2007), Factors controlling CO_2 exchange on timescales from hourly to decadal at Harvard Forest, *J. Geophys. Res.*, *112*, G02020, doi:10.1029/2006JG000293.

Vitasse, Y., A. J. Porte, A. Kremer, R. Michalet, and S. Delzon (2009), Responses of canopy duration to temperature changes in four temperate tree species: Relative contributions of spring and autumn leaf phenology, *Oecologia*, *161*, 187–198.

White, M. A., et al. (2009), Intercomparison, interpretation, and assessment of spring phenology in North America estimated from remote sensing for 1982–2006, *Global Change Biol.*, *15*, 2335–2359.

Yadav, V., K. L. Mueller, D. Dragoni, and A. M. Michalak (2010), A geostatistical synthesis study of factors affecting gross primary productivity in various ecosystems of North America, *Biogeosciences Discuss.*, *7*, 1445–1487, doi:10.5194/bgd-7-1445-2010.

Yuan, W., et al. (2009), Latitudinal patterns of magnitude and interannual variability in net ecosystem exchange regulated by biological and environmental variables, *Global Change Biol.*, *15*, 2905–2920, doi:10.1111/j.1365-2486.2009.01870.x.

A. R. Desai, Department of Atmospheric and Oceanic Sciences, University of Wisconsin-Madison, AOSS 1549, 1225 W. Dayton St., Madison, WI 53706, USA. (desai@aos.wisc.edu)